Characterisation of applied tensile stress using domain wall dynamic behavior of grain-oriented electrical steel

Article *in* Journal of Magnetism and Magnetic Materials · February 2017

DOI: 10.1016/j.jmmm.2017.01.076

CITATIONS
0

READS
34

4 authors, including:

Fasheng Qiu
University of Electronic Science and Technol…
3 PUBLICATIONS **2** CITATIONS
SEE PROFILE

Gui Yun Tian
Newcastle University
342 PUBLICATIONS **4,443** CITATIONS
SEE PROFILE

Bin Gao
University of Electronic Science and Technol…
70 PUBLICATIONS **578** CITATIONS
SEE PROFILE

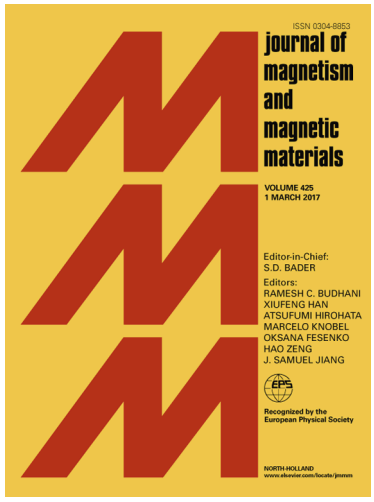

Characterisation of applied tensile stress using domain wall dynamic behavior of grain-oriented electrical steel

Fasheng Qiu, Wenwei Ren, Gui Yun Tian, Bin Gao

PII: S0304-8853(16)31738-3
DOI: http://dx.doi.org/10.1016/j.jmmm.2017.01.076
Reference: MAGMA 62428

To appear in: *Journal of Magnetism and Magnetic Materials*

Received Date: 9 August 2016
Revised Date: 7 November 2016
Accepted Date: 30 January 2017

Please cite this article as: F. Qiu, W. Ren, G.Y. Tian, B. Gao, Characterisation of applied tensile stress using domain wall dynamic behavior of grain-oriented electrical steel, *Journal of Magnetism and Magnetic Materials* (2017), doi: http://dx.doi.org/10.1016/j.jmmm.2017.01.076

Characterisation of applied tensile stress using domain wall dynamic behavior of grain-oriented electrical steel

Fasheng Qiu[1], Wenwei Ren[1,*], Gui Yun Tian[1,2,*], Bin Gao[1]
[1]School of Automation Engineering, University of Electronic Science and Technology of China, Chengdu, China
[2]School of Electrical and Electronic Engineering, Newcastle University, UK
*Corresponding authors: kgwrww@uestc.edu.cn, g.y.tian@ncl.ac.uk

ABSTRACT

Stress measurement that provides early indication of stress status has become increasingly demanding in the field of Non-destructive testing and evaluation (NDT&E). Bridging the correlation between micro magnetic properties and the applied tensile stress is the first conceptual step to come up with a new method of non-destructive testing. This study investigates the characterization of applied tensile stress with in-situ magnetic domain imaging and their dynamic behaviors by using magneto-optical Kerr effect (MOKE) microscopy assisted with magneto-optical indicator film (MOIF). Threshold magnetic field (TMF) feature to reflect 180^o domain wall (DW) characteristics behaviors in different grains is proposed for stress detection. It is verified that TMF is a threshold feature with better sensitivity and brings linear correlation for stress characterization in comparison to classical coercive field, remanent magnetization, hysteresis loss and permeability parameters. The results indicate that, 180^o DW dynamic in the inner grain is highly correlated with stress. The DW dynamics of turn over (TO) tests for different grains is studied to illustrate the repeatability of TMF. Experimental tests of high permeability grain oriented (HGO) electrical steels under stress loading have been conducted to verify this study.

Keywords: magneto-optical Kerr effect (MOKE) microscopy, magneto optical indicator film (MOIF), tensile stress, domain wall (DW) dynamic behavior, threshold magnetic field (TMF)

1. Introduction

Different electromagnetic non-destructive testing and evaluation (NDT&E) methods including integration of macro and micro magnetics have been applied for stress characterization [1-5]. Magnetic hysteresis loop technique is one of the typical macroscopic NDT&E methods to characterize the stress in ferromagnetic test object [1, 2, 6]. The correlation between mechanical stress and the major/ minor hysteresis loop has been widely studied by many researchers[6, 7]. The features extracted from magnetic hysteresis loops e.g. the coercive field, remanent magnetization and hysteresis loss have been conducted to characterize stress status of ferromagnetic object[6, 8, 9]. Dobmann[10] applied the 3MA methods to characterize the applied and residual stress of steel through multi-parameters of macroscopic magnetic detection signals. However, the macro B-H curves reflecting the average magnetic response in different areas has a low spatial resolution for stress assessment. Moreover,

classical magnetic properties (e.g. coercivity, remanent magnetization, hysteresis loss, permeability) from global B-H loops are unable to detect small stress variation because of relative low sensitivity and non-linearity.

Due to the progress in magnetic microstructure observation techniques, dynamic characteristics of DW is becoming a topic of interest not only due to its potential applications to magnetic memory, logic devices and soft magnetic materials[11-14], but also because of the fascinating future for the high spatial resolution[8, 9, 15, 16] measurement of stress in ferromagnetic materials. Perevertov et al.[8, 9] revealed that the tensile stress removes the closure domains of grain oriented Fe-3%Si steel. Klimczyk et al.[17] reported that cutting stress induced the creation of a surface magnetic domain stress pattern. Batista et al.[18, 19] studied DW interactions with cementite precipitate along with macro magnetic responses. The above researches of DW dynamic behavior are confined in the discussion of qualitative analysis. However, the quantitative analyses are essential for stress measurement. Qiu et al.[15] and Gao et al. [16] employed DW motion velocity feature to evaluate the tensile stress in electrical steel. Threshold based magnetic / current field features are widely used for the investigation of DW propagation characteristics under pinning condition [11-14, 20]. It is verified that the threshold field value has linear relationship with pinning potential [11, 13, 21]. This work extends threshold field feature for stress evaluation.

Grain-oriented electrical steels are extensively used in industry e.g. electrical transformers and motors. During production, an insulating surface coating are applied on the electrical steel to prevent corrosion, avoid planar eddy currents and reduce magnetic loss [22, 23], and it is easy to induce beneficial stress and residual stress in the object. Residual stress with applied beneficial loading has a strong influence on DW movement[23]. To evaluate the stress in the electrical steel, in-situ inspection of magnetic microstructure and their correlation with stress status is timely required. However, the samples preparation e.g. polishing process is a critical issue for magnetic microstructure observation technique. Both bulk magnetic properties and magnetic microstructure are sensitive to insulating surface coating on the electrical steel [22-24]. This limits in-situ measurement of magnetic domain. Richert et al.[25] proposed an approach for direct domain texture observation by using MOKE microscopy with the help of MOIF. This paper extends the method for stress characterization. The 180^{o} DWs behavior of a coated grain-oriented electrical steel under different levels of tensile stress along the [001] direction are measured. The relationship between the behavior of magnetic dynamic domainsand applied tensile stress is investigated. Specifically, surface hysteresis loop considering the 180^{o} DW motion are reported for stress assessment. Threshold magnetic field (TMF), where all 180^{o} DW propagation is finished, is measured under different levels of stress. It is verified that the TMF feature has better sensitivity and linearity for stress evaluation.

This paper is organized as follows: Section 2 introduces the magnetic microstructure observation using the hybrid MOKE with MOIF for the grain boundary (GB) and magnetic domain observation. Section 3 reports experimental results analysis including dynamic 180^{o} DW behaviors, TMF feature and B-H curve for stress evaluation. Finally, the conclusions and future work are given in Section 4.

2. Methodology

2.1Hybrid MOKE with MOIF for microstructure observation

MOKE with assistance of MOIF technique is an indirect imaging method based on the magneto-optical Faraday Effect for the visualization of magnetic stray fields and domains of magnetic materials[25, 26]. The magneto-optical Faraday Effect is an interaction between polarized light and a transparent magneto-optical garnet film[26-28], which causes a rotation of the plane of polarization in correspondence with the magnetic field strength. The film with out-of-plane anisotropy has an easy axis of magnetization normal to the sensor surface to make them sensitive to vertical magnetic fields. The magnetic domain structure of the MOIF without magnetic field in the space is shown in Fig. 1(a). It suggests that the total area of light and dark domains is equal. This can be sketched in Fig 1(b). When the MOIF is placed onto the surface of magnetic materials, there has to be a small out of plane component of magnetization in the materials that causes surface poles and thus emerging a stray field [25, 29] as shown in Fig. 2(a). Then the perpendicular component of the field expands / narrows the area of domains which is parallel / antiparallel to the direction of the field which is shown in Figs. 1(c) and 1(d). The local magnetization in the MOIF is changed which induces variations in Faraday rotation signal. With overview window Kerr microscopy[27], the Faraday rotation signal is averaged. An analyzer is used to detect optical contrast corresponding to the rotation. In this case, the image looks like variations in the light and dark tones with the intensity corresponding to local magnetic domain pattern of the test sample. Magnetic domain imaging of a HGO sample under demagnetized state is presented in Fig. 2(b). In addition, hybrid MOKE with MOIF enables to visualize GB distribution as well as magnetic domain texture simultaneously. The GB separates two adjoining grains with different crystal orientation. Both width and orientation of magnetic domains vary with each grain. As a result, profile of GB can be imaged in demagnetized state. This can be seen in Fig. 2(b). The magnetic field leakage around the GB is significantly higher than in the grain interior when the sample is magnetized. The larger stray field around GB induces larger Faraday signal, leading brighter or darker intensity in the magnetic domain image. Therefore, the shape of GB is mapped although the magnetic domains are in saturation state. The GB profile of HGO sample at a specific field of 880 A m^{-1} is presented in Fig. 2(c). Based on the setup and observation, dynamic behaviors of DW can be captured and characterized for stress characterization.

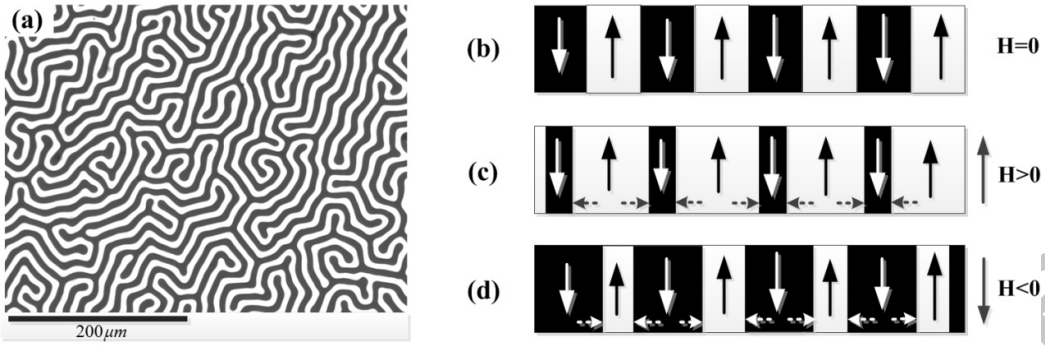

Fig.1. (a) Magnetic domain pattern of the magneto-optical garnet film, imaged by Faraday microscopy in a polarizing microscopy; Lateral schematic of domains (b) without magnetic field; (c) with a upward magnetic field; (d) with a downward magnetic field

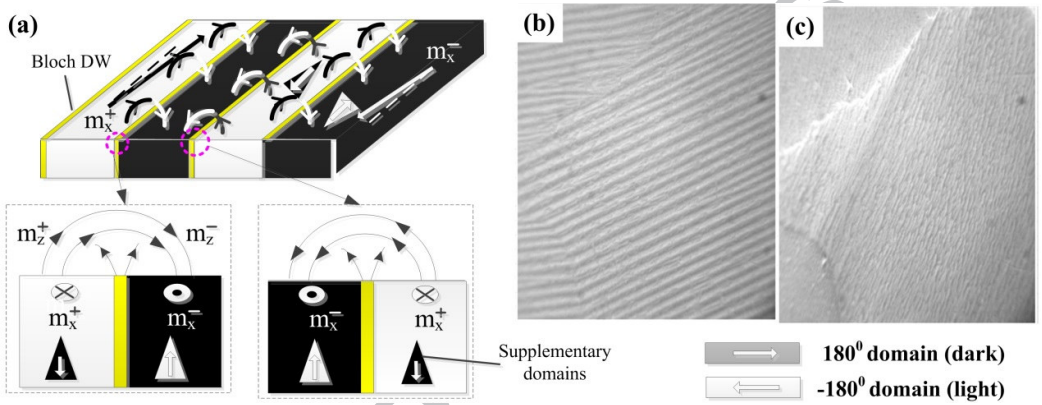

Fig. 2.(a) Magnetic stray field caused by the surface poles generating from a small out of plane component of magnetization [29], where the m_x and m_z are in-plane and out-of-plane magnetization components, respectively; (b) Magnetic domains of high permeability grain-oriented (HGO) electrical steel in demagnetized state; (c) GB profile of HGO at a magnetic field of 880 Am^{-1} where the dimension of the domain pattern picture is 16.19×10.78 mm^2

2.2 Experiment set-up and sample preparation

To observe the GB and domain textures of steels, three samples of HGO electrical steel are employed for the experimental studies. This material usually has a silicon content of 3% by mass. To avoid corrosion and planar eddy currents, an insulating coating has been applied on the sample surface. The geometrical size of the three samples is 300mm× 30mm× 0.27 mm shown as Fig. 3. In this experiment, the steels were applied to an elastically tensile stress up to approximately 61.9 MPa along the rolling direction {0 0 1}.

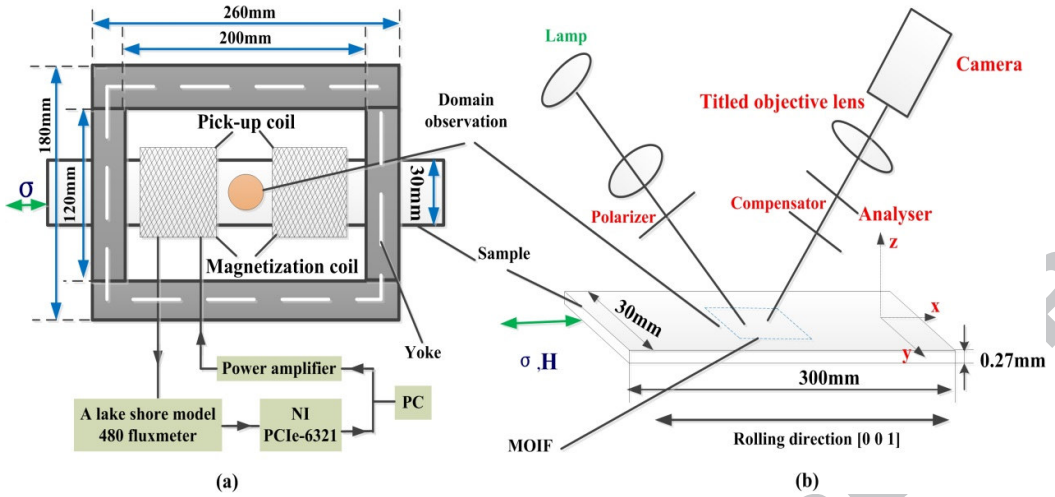

Fig. 3. (a) Sketch of the measurement set-up; (b) Principal scheme of MOKE plus MOIF

A MOKE microscopy with the assistance of MOIF (dimensional: 20mm×15 mm) is employed for visualization of DWs and GB. Fig. 3(a) illustrates the experimental setup including magnetization configuration, pick-up coils, and applied loading of tensile stress. Fig. 3(b) shows the schematic diagram of the MOKE microscopy system associated with MOIF for observation of magnetic domain and GB. In order to image magnetic domains during dynamic magnetization process, excitation coils with 355 turns wound around sample were used to generate magnetic field with wire diameter of 0.8 mm and wire impedance of 1.8 Ohms, and we calculated the internal field from the current in the magnetization coil. The magnetic laminated yoke was used to close the magnetic flux path. During test, the pickup coil with 363 turns is used to detect the changes of induced voltage inside the sample to find B and H with wire diameter of 0.2 mm and wire impedance of 29 Ohms. A lake shore model 480 flux meter is applied to calculate the magnetic flux by integration of the induced voltage at the pick-up coil.

In this experiment, the sample was demagnetized in a slowly decaying field at 0.01Hz. The testing was done by using a triangular field waveform with field amplitude of 1000 A m^{-1}. The magnetization frequency was 0.01Hz to stabilize the response in the quasi-static regime. The magnetic microstructures of domain patterns and GB were observed by a longitudinal MOKE microscopy assisted with MOIF. The images of domain textures are captured and recorded by a digital CCD camera, C8484-03G02 with sampling rate of 16.3 Hz. To obtain GB distribution and DW behavior for different grains, the images of domain pattern and GB are obtained separately for each measured areas by moving MOIF. The grain profile, grain size and its distribution of the sample are plotted in the Fig. 4 through edge detection of images from the MOIF. Different grains' DW behaviors and their features for same applied stresses will be studied and compared with conventional hysteresis loops based macro parameters.

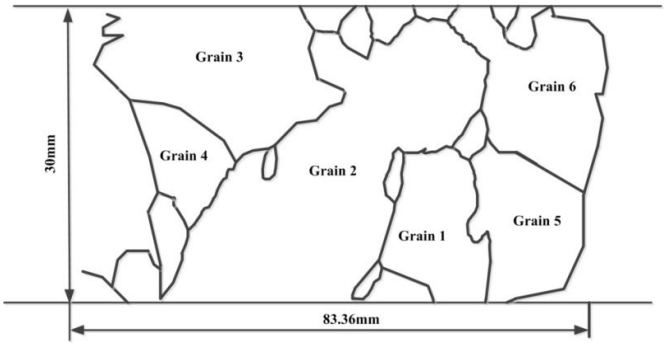

Fig. 4. Grain size and its distribution of the sampleS1

3. Result and discussion

MOKE in conjunction with MOIF has been applied for microstructure observation of the HGO steels under different levels of tensile stresses. TMF is proposed for stress characterization. Difference of 180^o DWs characterization in response to stress for different grains and different samples is studied. Further, the difference of TMF of TO tests for different grains is investigated to illustrate the repeatability of TMF behaviors.

3.1 Proposed TMF feature considering 180^o DW dynamic behaviors for stress evaluation

Figs.5-7 present the surface magnetic domain pattern under different magnetic field plus tensile stress for the descending branch of B-H loops in grain 1 of sample S1. At a magnetic field of 177 A m^{-1}, all the 180^o and -180^o magnetic domains orient at 180^o direction at zero stress or at a stress of 30.9 MPa which are shown in Figs. 5(a) and 6(a). A few -180^o domains appear when the stress grows to 61.9MPa are shown in Fig. 7(a). As the field strength is decreased to 25 A m^{-1}, all the domains still retain in 180^o direction when the applied tensile stress is zero as shown in Fig. 5(b). In contrast, many -180^o domains are observed under a tensile stress of 30.9 MPa as displayed in Fig. 6(b), and the area of -180^o magnetic domains is expanded when the stress grows to 61.9 MPa which is shown in Fig. 7(b). As the magnetic field reduces to zero (Remanent state), -180^o magnetic domains appear at zero stress which is presented in Fig. 5(c). -180^o magnetic domains are expanded and 180^o magnetic domains are narrowed at a stress of 30.9 MPa and 61.9 MPa, respectively. This can be seen in Figs. 6(c) and 7(c) respectively. The demagnetizing effect hinders 180^o DWs motion under tensile loading [8]. Therefore, higher magnetic field strength needs to be applied to make all the 180^o DWs displacement finished.

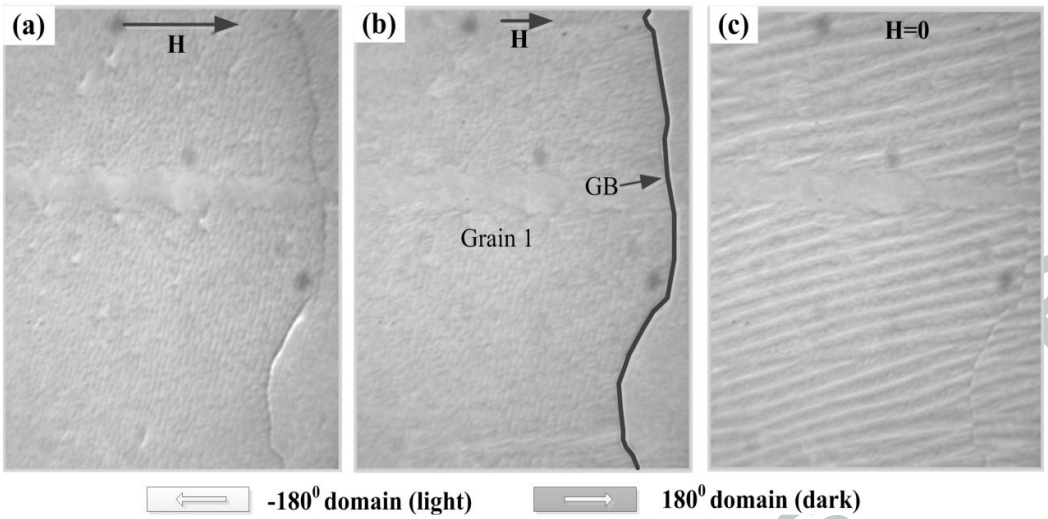

Fig. 5. The magnetic domain patterns in grain 1 from descending branch for zero stress on the sample 1 (a) At 177Am^{-1}; (b) At 25 Am^{-1}; (c) At 0 Am^{-1}, where the size of the pictures is 10.47 mm$\times$8.52 mm.

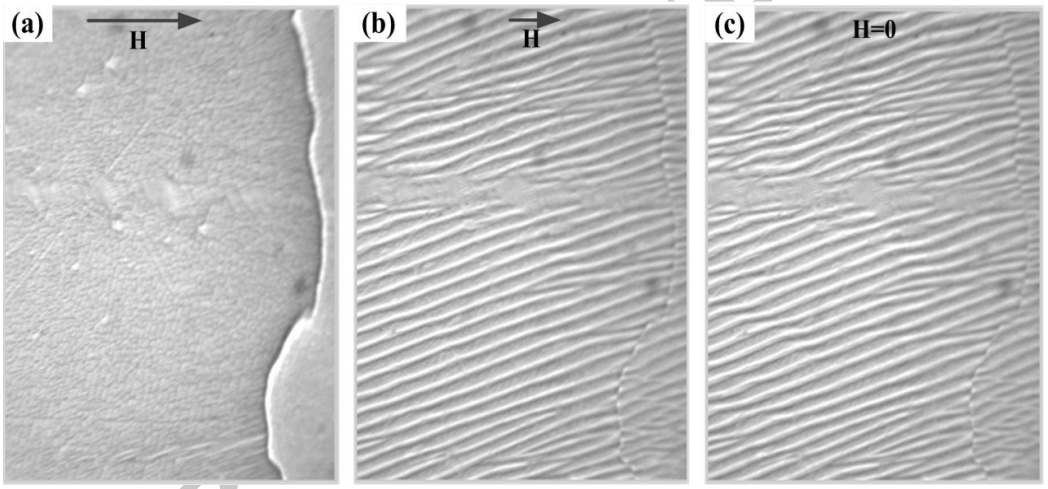

Fig. 6. The same as Fig.5 with a tensile stress of 30.9 MPa

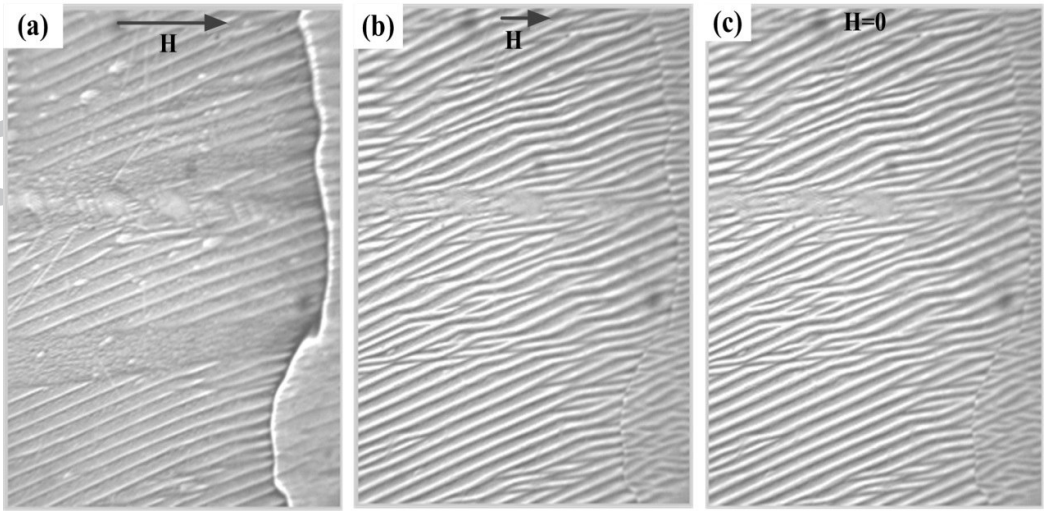

Fig. 7. The same as Fig.5 with a tensile stress of 61.9 MPa

To quantitatively estimate the stress in the grain, the relationship between stress and DW dynamic characterization is established. We consider 180^{o} surface DWs displacement under different magnetic field strengths. The areas of surface 180^{o} and -180^{o} magnetic domains variation which can reflect 180^{o} DW propagation characteristics and it can be expressed as:

$$S_{Nom} = \frac{S_{180^0}^{total} - S_{-180^0}^{total}}{S_{180^0}^{total} + S_{-180^0}^{total}} \quad (1)$$

where $S_{180^0}^{total}$ and $S_{-180^0}^{total}$ represent the total areas of 180^{o} and -180^{o} domains, respectively. In the demagnetized state, $S_{180^0}^{total}$ is equal to $S_{-180^0}^{total}$, and S_{Nom} is zero. If a magnetic field H is applied on the sample, the 180^{o} DWs abruptly displace some distance discontinuously to a position with the minimum energy state. The 180^{o} DWs movement is completed at a specific TMF value. Meanwhile, all 180^{o} and -180^{o} magnetic domain orient at 180^{o} (-180^{o}) direction and S_{Nom} is +1 (-1).As the magnetic field strength exceeds the TMF value, only the magnetic domain rotation contributes to the magnetization process. The 180^{o} and -180^{o} DWs motion process is not only influenced by external factors (e.g. applied stress, temperature and deformation, etc.), but also related to the intrinsic factor (e.g. lattice defects, intrinsic pinning sites and anisotropy, etc.). Hence, the TMF feature highly depends on the individually studied area. This feature is used to detect local magnetic characteristic for stress assessment. TMF value can be obtained when S_{Nom} becomes +1 or -1. In this work, we calculated the TMFs in the major grains for the observation area to understand the differences and robustness.

The profile of S_{Nom}-H curve in grain 1 at zero stress is shown in Fig. 8(a) where all the values are normalized. From the descending branch of the S_{Nom}-H curve at zero stress, all 180^{o} DWs displacement is completed when magnetic field exceeds 25Am^{-1} or lower than -78 A m^{-1}. When -78 A m^{-1}< H < 25 A m^{-1}, 180^{o} DWs motion occur. As $H \geq 25$ A m^{-1} $(H \leq -78$ A m$^{-1})$, all 180^{o} and -180^{o} magnetic domain are aligned in 180^{o} (-180^{o}) direction.

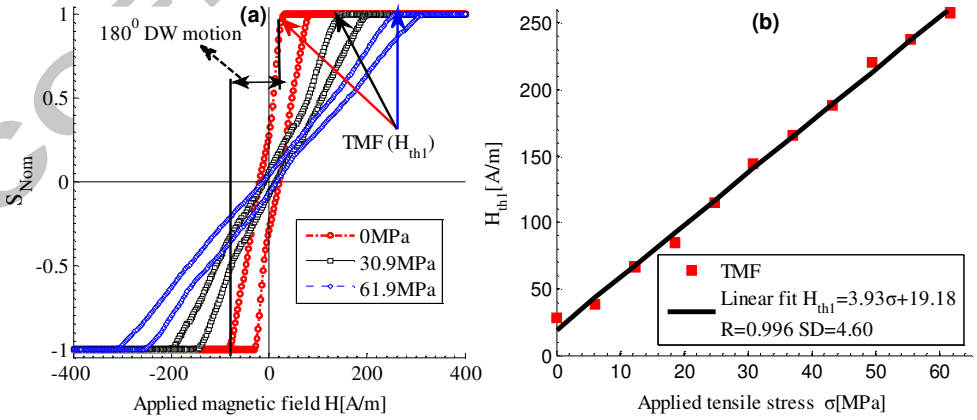

Fig. 8. (a) S_{Nom}–H loops under tensile stress for grain 1 on the sample S1; (b) Correlation of TMF (H_{th1}) with stress, where R is Pearson's correlation coefficient and SD is the standard deviation of the linear fit.

With different applied tensile stresses, the profile of S_{Nom}-H curves are calculated and shown in Figs. 8(a).With increasing stresses, S_{Nom}-H curves become constrict and flat. The TMF value shifts to higher values as the stresses increase. It can be noticed that the TMF for grain 1 from the descending branch in the first quadrant, TMF is 23 A m^{-1} at zero stress, and as the stress grows up to 61.9 MPa, TMF is 258 A m^{-1}. With different levels of stress, H_{th1} is measured and plotted in the Fig. 8(b) for linearity analysis. It is shown that H_{th1} has a linear relationship with applied stress with a slope of 3.93 A m^{-1} per MPa. The quantitative fitted formula can be expressed as: $H_{\mathrm{th1}} = 3.93 * \sigma + 19.18$.

TMF is a feature for contrast of DW movement. When a tensile stress is applied parallel to a 180^0 wall the domains on either side grow at the expense of the 90^0 closure domains, increasing the length of 180^0 wall. However, with a perpendicular magnetic field, the only contribution to the permeability comes from the 90^0 walls and so permeability is decreased compared to the unloaded state. For a tensile stress applied perpendicular to a 180^0 wall the closure domains at each end grow, decreasing the length of 180^0 wall. It means the changes will depend on the grain orientation and DW configuration including orientation to any stress.

3.2 Difference of TMF for different grains

Figs. 9(a)-9(c) and Figs. 10(a)-10(c) present the magnetic domain pattern at a magnetic field of 25 A m^{-1} from descending branch for grains 1 and 2, respectively. At zero stress, all the 180^o and -180^o magnetic domains orient 180^o direction and this is presented in Fig. 5(a). In contrast, a few -180^o domains exist for grains 2 and 3 as shown in Figs. 9(a) and 10(a). Figs. 9(c) and 10(c) present that the width of -180^o magnetic domains in grains 3 is higher than grain 1 and 2 at 30.9 MPa or 61.9 MPa. It can be drawn that the 180^o DWs dynamic behaviors vary with different grain region.

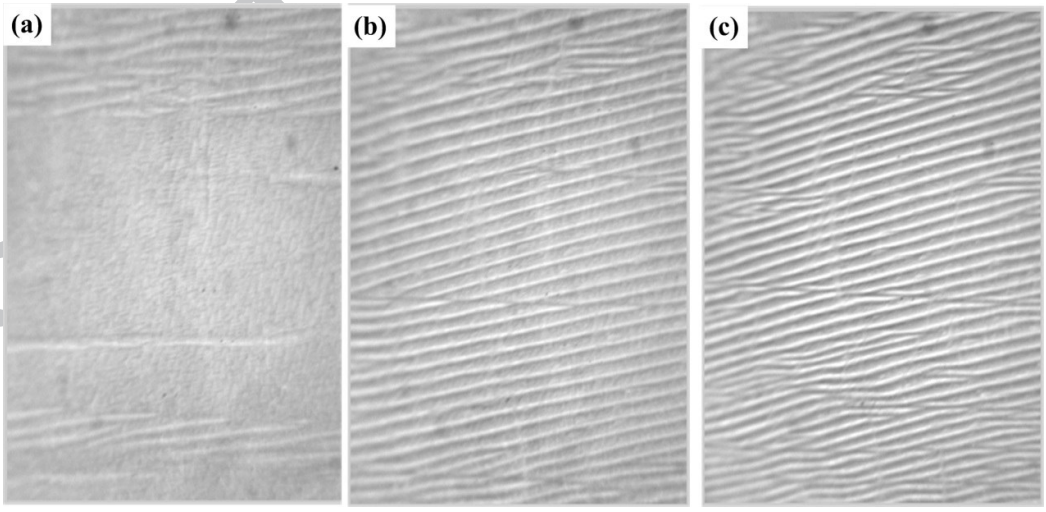

Fig. 9. The magnetic domain patterns for grain 2 on sample S1from descending branch at 25 A m^{-1} (a) At 0 MPa;(b) At 30.9 MPa; (c) At 61.9 MPa, where the size of the pictures is 17.31×9.9 mm^2.

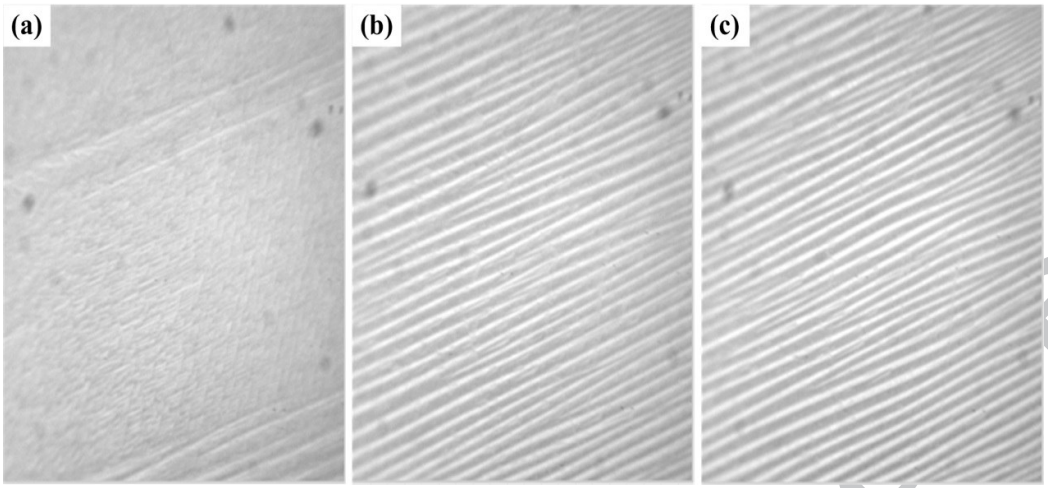

Fig. 10. The magnetic domain patterns for grain 3 on sample S1 from descending branch at 25 A m^{-1}(a) At 0 MPa;(b) At 30.9 MPa; (c) At 61.9 MPa, where the size of the pictures is 14.15×10.23 mm^2.

Figs. 11(a) and 12(a) present S_{Nom}-H loops under different levels of stress for the grains 2 and 3, respectively. The shape of loops for different grains at the same stress has significant differences in term of the smoothness and slope. S_{Nom}-H curves for the grain 2 have a higher average slope than those of grains 1 and 3 under 61.9 MPa. S_{Nom}-H curves for the grain 3 are more smooth than grain 1 and 2 at 0 MPa, 31.5 MPa and 61.9 MPa, which reflects 180° DWs smooth movement in response to magnetic field. Figs. 11(b) and 12(b) present relationship between TMF and stress for the grains 2 and 3, respectively. It can be seen that TMFs for the grains 2 and 3 are linearly correlated as stress increase. The correlation coefficient is 2.97 A m^{-1} per MPa for the grain 2 and 3.80 A m^{-1} per MPa for the grain 3. The quantitative fitted formulas are estimated by: $H_{th2} = 2.97 * \sigma + 32.91$ for the grain 2 and $H_{th3} = 3.80 * \boldsymbol{\sigma} + \mathbf{28.14}$ for the grain 3.

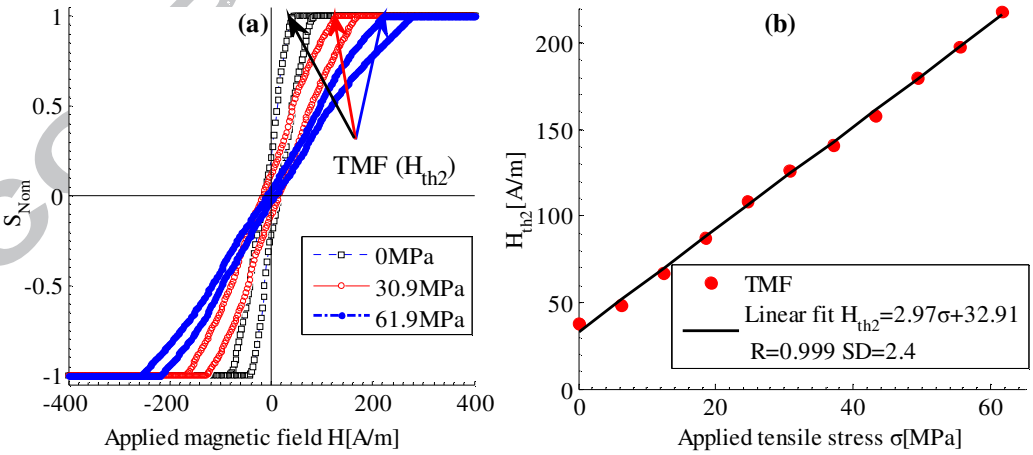

Fig. 11. (a) S_{Nom}–H loops under tensile stress for grain 2 on sample S1; (b) Correlation of TMF (H_{th2}) with stress.

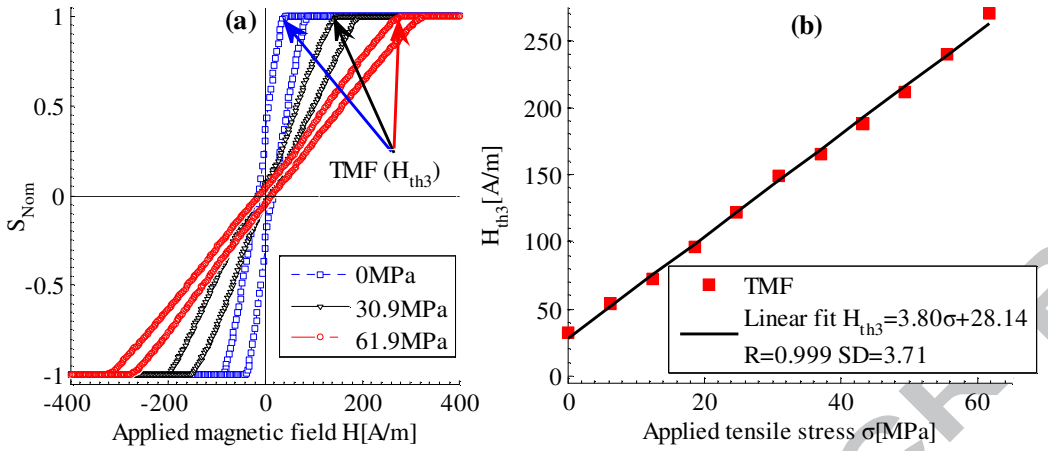

Fig. 12.(a) S_{Nom}–H loops under tensile stress for grain 3 on sample S1; (b) Correlation of TMF (H_{th3}) with stress.

For the grains 4-6, the 180^{o} DWs dynamic behaviors, S_{Nom}-H loops and TMFs, are measured. TMFs in grains 4-6 also have linearly correlation with stress. Average TMF value ($\overline{H}_{th}$) with grains 1-6 is calculated, and its correlation with tensile stress is shown in Fig. 13(a). The quantitative fitted formula is given by: $\overline{H}_{\text{th}} = \mathbf{3.57} * \sigma + \mathbf{26.74}$. This quantitative fitted relationship can be used to further predict macro applied tensile stress.

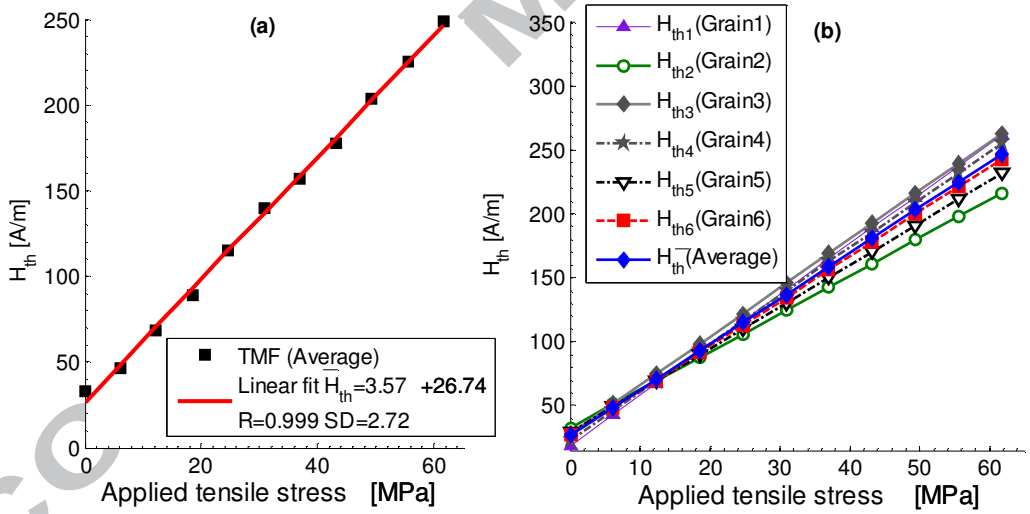

Fig. 13. (a) Correlation of average TMF with stress for sample S1; (b) Difference in fitting TMF in different grains for sample S1.

With different grains, the difference in fitting TMF is presented Fig. 13(b). It is shown that the slopes of linear fitting are different from grain to its neighbor. Moreover, the TMF values have slight difference with different grains at the same amount of applied stress. For the fitting function in grains 1-6, the offset ranges are from 19 A m^{-1} to 32.9 A m^{-1}, and the slope ranges are from 2.97 A m^{-1} per MPa to 3.93 A m^{-1} per MPa. Difference of 180^{o} DWs behavior, S_{Nom}-H loops and TMF with different

grains can be interpreted as: 1) Although HGO electrical steels have a $\{110\}\langle 001\rangle$ preferred crystal orientations, the orientation deviations from the ideal Goss orientation lie in the range off about 7^{o} for conventional grain-oriented steel and in the range of about 3^{o} for high permeability grades[30]. Hence, TMFs under different grains have a difference of 20% under tensile stresses linking to the characters of grains, which opens a field for further quantitative investigation of grain orientation using TMF. 2) To avoid the eddy current between lamination, an insulating coating is applied to the surface of HGO electrical steels [22, 23]. Meanwhile, residual stress is generated at the surface of the sample. The remaining residual stress distribution is different in each grain [31], causing variations in local macro magnetic properties, 180^{o} DWs dynamic behaviors, initial TMF value without applying mechanical stress; 3) With applied loading, the sample leads to a state of macrostress, and the microstress is supported by each grain. Intergranular strains within those grains are related to residual stress [31], grain orientation [31, 32]. The intergranular strains, which interacted via the magnetostriction with the magnetic moments to provide local energy barriers for the 180^{o} DW motion, are inhomogeneous. This may induces the TMF difference.

3.3 Difference of TMF of TO tests for different grains

To illustrate the repeatability of TMF, the TO tests of the DW dynamic were conducted. Figs. 14(a)-(c) present the TO magnetic domain pattern at a magnetic field 25 A m^{-1} from the descending branch in grains 1, 2 and 3, respectively. Due to the large grain size in HGO steels, the magnetic domains in the cross section of the sample are laid in the same grain. Although the DW orientation changes when the sample is turned over, the domain patterns at the upper surface and lower surface have small difference at same magnetic field and stress.

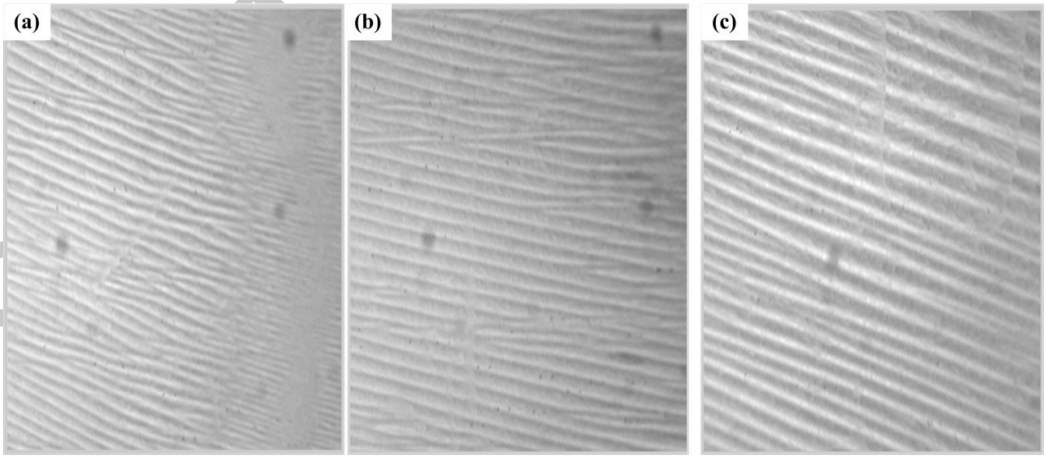

Fig. 14. Magnetic domain pattern of turn over tests at a magnetic field of 25 A m^{-1} under 30.9 MPa loading for different grains (a) In grain 1; (b) In grain 2; (c) In grain 3, where the size of the pictures is 10.47×8.52 mm^2

The TMF values of TO tests for grains 1, 2, 3 under different loading are measured, and their correlations with stress were shown in Figs. 15(a), 15(b) and 15(c). The quantitative fitted formulas are estimated by: $H_{\mathrm{th1}}^{\mathrm{TO}} = 3.95*\sigma + 19.36$ for the grain 1, $H_{\mathrm{th2}}^{\mathrm{TO}} = 2.99*\sigma + 32.54$ for the grain 2, $H_{\mathrm{th3}}^{\mathrm{TO}} = 3.76*\sigma + 30.23$ for the grain 3. The TMFs, slope and offset ranges in the fitting function have

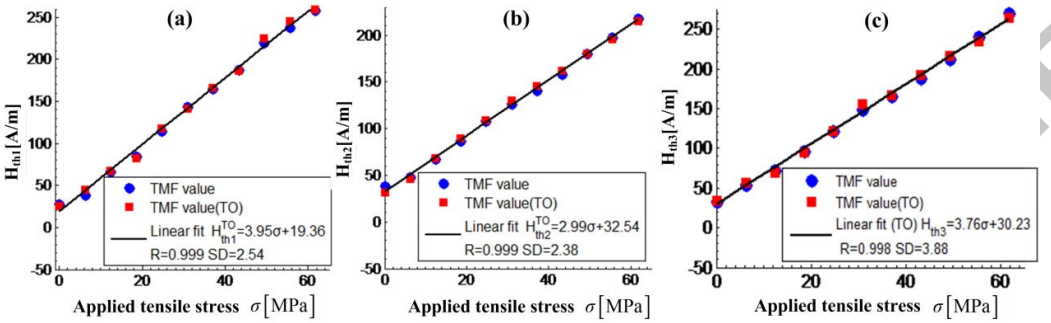

less than 10% difference, which illustrates the good repeatability TMF for stress evaluation.

Fig. 15. Difference of TMF of TO tests for different grains (a) In grain 1; (b) In grain 2; (c) In grain 3

The experimental tests were validated on two extra test samples. Fig. 16 presents the relationship between fitting average TMF value and stress for different samples. The quantitative fitted formulas can be expressed as: $\overline{H}_{th} = 3.46*\sigma + 15.23$ for sample S2 and $\overline{H}_{th} = 3.30*\sigma + 20.55$ for sample S3. The slopes of the fitting average TMF for different samples have a difference less than 5%, while there exists great difference in offset. This may have caused by the difference of average residual stress and grain boundaries on the surface of the samples, which will be further studied.

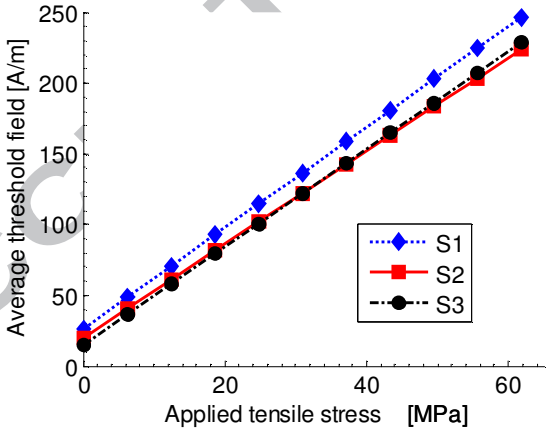

Fig. 16. Difference in fitting average TMF value with samples S1, S2 and S3

3.4 TMF for global stress characterization

Fig. 17(a) shows the magnetization curves of the HGO electrical steel S1. With different applied stress, coercivity, remanent magnetization, hysteresis loss, maximum differential permeability and

fitting average TMF value are normalized and presented in Fig. 17(b). Coercivity increases by 7.1% stress ranges from 0 MPa to 18.5 MPa and then decreases by 16.2% as stress increases to 61.5MPa. As the stress is 0 MPa to 61.9 MPa, hysteresis loss and maximum differential permeability decrease monotonically by 17% and 61%, respectively. Coercivity, hysteresis loss and maximum differential permeability change with average slopes of 0.37% per MPa, 0.27% per MPa and 0.98% per MPa, respectively. Remanent magnetization decreases at low stress by 61.5% and beyond bout about 12.3 MPa it decrease 18.1%. The remanent magnetization reduces rapidly with an average slope of 3.3% per MPa as stress ranges from 0 MPa to 12.3 MPa. However, remanent changes slightly with an average rate of 0.38% per MPa when stress is in the range of 12.3 MPa - 61.9 MPa. Coercivity and hysteresis loss cannot be used for evaluating stress because of low sensitivity. Remanent magnetization is effective in detecting small stress, but incapable of determining high stress. Average TMF increases by 89.4% when stress increases from 0 MPa to 61.9 MPa, and the increase is linear correlated with a slope of 1.44% per MPa. Compare with coercivity, remanent magnetization, hysteresis loss and maximum differential permeability, the average TMF has a wider variation range and good linear relationship behavior for applied global stress characterization. Furthermore, it provides more accurate assessment of small stress variation which improves the accuracy of mechanical degradation of engineering structures in operational plant.

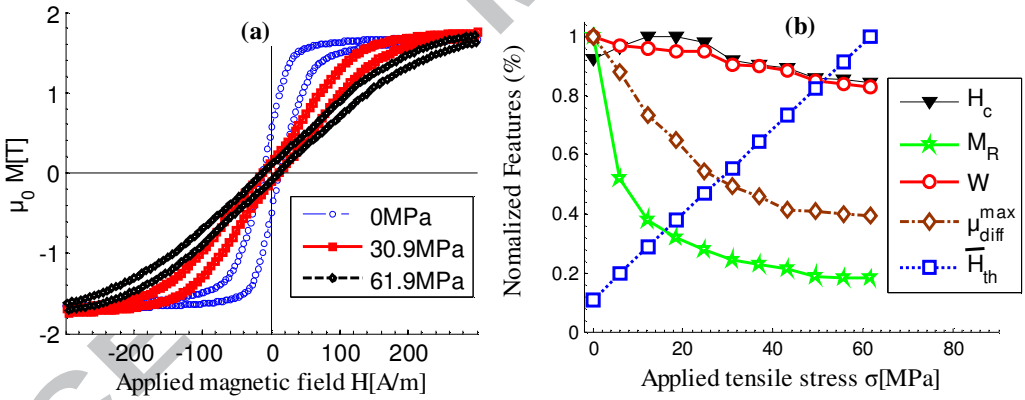

Fig. 17. (a) Bulk B-H loops under different levels of stresses for sample S1; (b) Normalized features [coercivity (H_c), remanent magnetization (M_R), hysteresis loss (W), maximum differential permeability (μ_{diff}^{max}) and fitting average TMF value ($\overline{H}_{th}$)] as a function of stress for samples S1.

4. Conclusion and future work

This work was performed to study the effect of tensile stress on magnetic 180^{o} DWs dynamic behaviors in grain-oriented electrical steel without treatment based on MOKE combining with MOIF. S_{Nom}-H curves considering the 180^{o} DW motion under different levels of stress were measured. The conclusions are drawn as follows: 1) Magnetic domain pattern observations have shown that applied tensile stress blocks the 180^{o} DWs motion. Once all the 180^{o} DWs displacement is completed, TMF

appears at higher applied magnetic field strength with higher stress; 2) TMF is proposed for stress and local 180^{o} DW dynamic characterizations in grain level. This new feature has a linear relationship with stress variation in each grain. However, the offsets and slopes of the linear fitting lines have slight differences for different grains. This may result from the grain orientation deviation, complex residual stress distribution; 3) The turn over measurement of DW dynamics illustrates good repeatability TMF against applied stress within the variation of 10% for the same grains; 4) Average TMF $\bar{H}_{th}$ increases by 89.3% when the stress ranges 0-61.9 MPa. And the increase is linear with an average slope of 3.57 A m^{-1} per MPa. Compared with coercivity, remanent magnetization, hysteresis loss and maximum differential permeability, average TMF shows its better sensitivity and linearity to measure global applied stress and small stress variation.

MOKE with the help of MOIF for mapping of GB and magnetic domains can be potentially used as a measure to assess the local stress concentration, microstress, residual stress, micro defect as well as quality control of materials without any treatment in real time. Understanding the interaction between 180^{o} DWs dynamic behaviors and applied mechanical stress is important for the future development of high performance electro-magnetic materials. The shortcoming of MOKE plus MOIF system includes:1) the MOIF used in this study can only be used in overview Kerr microscopy because of the relatively larger domain size in the MOIF; 2) Compared with MOKE technique for stress measurement, MOKE with MOIF method only considers the 180^{o} DW motion process, and domain rotation process is unable to be determined.

Future research in conjunction with 180^{o} DW dynamics [33] will include:1) Correlation between grain orientation and TMF will be further investigated to understand the difference Of TMF in different grains and their domain width measurements and influences including the additional domains that can be seen for the higher stress case rather than a change in domain width; 2) Residual stress distribution and intergranular microstress in each grain under the applied tensile stress will be explored through TMF features and their character; 3) The correlation between S_{Nom}-H curves and macro B-H curves will be studied for micro and marco stress characterisation.

Acknowledgement

We acknowledge the financial sponsored by the National Natural Science Foundation of China (Grants No.51377015 and No.61527803), and partially funded by EPSRC UK-China collaborative project (EP/F06151X/1). The authors would like to Yunlai Gao in the Newcastle University, UK, Ms. JiaLiu, Peng Lu, Kun Zeng in the University of Electronic Science and Technology of China, and Professor R. Schäfer in the Institute of Metallic from IFW Dresden, Germany for the useful discussion.

Reference

[1] N. Kasai, H. Koshino, K. Sekine, H. Kihira, M. Takahashi, Study on the effect of elastic stress and

microstructure of low carbon steels on Barkhausen noise, Journal of Nondestructive Evaluation, 32 (2013) 277-285.
[2] M. Fukuhara, T. Yonamine, F. Landgraf, F. Missell, Evolution of magnetic properties and crystallographic texture in electrical steel with large plastic deformation, Journal of Applied Physics, 109 (2011) 07A325.
[3] P. Wang, Y. Gao, Y. Yang, G. Tian, E. Yao, H. Wang, Experimental studies and new feature extractions of MBN for stress measurement on rail tracks, IEEE Transactions on Magnetics, 49 (2013) 4858-4864.
[4] S. Ding, G. Tian, V. Moorthy, P. Wang, New feature extraction for applied stress detection on ferromagnetic material using magnetic Barkhausen noise, Measurement, 73 (2015) 515-519.
[5] L. Guo, D. Shu, L. Yin, J. Chen, X. Qi, The effect of temperature on the average volume of Barkhausen jump on Q235 carbon steel, Journal of Magnetism and Magnetic Materials, 407 (2016) 262-265.
[6] O. Stupakov, I. Tomáš, Hysteresis minor loop analysis of plastically deformed low-carbon steel, NDT & E International, 39 (2006) 554-561.
[7] A. Ktena, D. Davino, C. Visone, E. Hristoforou, Stress dependent vector magnetic properties in electrical steel, Physica B: Condensed Matter, 435 (2014) 25-27.
[8] O. Perevertov, R. Schäfer, Influence of applied tensile stress on the hysteresis curve and magnetic domain structure of grain-oriented Fe–3% Si steel, Journal of Physics D: Applied Physics, 47 (2014) 185001.
[9] O. Perevertov, J. Thielsch, R. Schäfer, Effect of applied tensile stress on the hysteresis curve and magnetic domain structure of grain-oriented transverse Fe-3% Si steel, Journal of Magnetism and Magnetic Materials, 385 (2015) 358-367.
[10] G. Dobmann, I. Altpeter, B. Wolter, R. Kern, Industrial applications of 3MA–micromagnetic multiparameter microstructure and stress analysis, Electromagn. Nondestr. Eval.(XI), 31 (2008) 18-25.
[11] S. Lepadatu, A. Vanhaverbeke, D. Atkinson, R. Allenspach, C. Marrows, Dependence of domain-wall depinning threshold current on pinning profile, Physical review letters, 102 (2009) 127203.
[12] L. Thomas, M. Hayashi, X. Jiang, R. Moriya, C. Rettner, S.S. Parkin, Oscillatory dependence of current-driven magnetic domain wall motion on current pulse length, Nature, 443 (2006) 197-200.
[13] D. Ravelosona, S. Mangin, J. Katine, E.E. Fullerton, B. Terris, Threshold currents to move domain walls in films with perpendicular anisotropy, Applied physics letters, 90 (2007) 072508.
[14] T. Koyama, D. Chiba, K. Ueda, K. Kondou, H. Tanigawa, S. Fukami, T. Suzuki, N. Ohshima, N. Ishiwata, Y. Nakatani, Observation of the intrinsic pinning of a magnetic domain wall in a ferromagnetic nanowire, Nature materials, 10 (2011) 194-197.
[15] F. Qiu, W. Ren, G.Y. Tian, Y. Gao, B. Gao, The effect of stress on the domain wall behavior of high permeability grain-oriented electrical steel, 2015 IEEE Far East NDT New Technology & Application Forum (FENDT), IEEE, 2015, pp. 207-211.
[16] Y. Gao, G.Y. Tian, F. Qiu, P. Wang, W. Ren, B. Gao, Investigation of Magnetic Barkhausen Noise and Dynamic Domain Wall Behavior for Stress Measurement, 19th World Coneference on Non-Destructive Testing, Munich, Germany, 2016, pp. 1-7.
[17] P.K. Klimczyk, P. Anderson, A. Moses, M. Davies, Influence of cutting techniques on magnetostriction under stress of grain oriented electrical steel, Magnetics, IEEE Transactions on, 48 (2012) 1417-1420.
[18] L. Batista, U. Rabe, S. Hirsekorn, Magnetic micro-and nanostructures of unalloyed steels: Domain wall interactions with cementite precipitates observed by MFM, Ndt & E International, 57 (2013) 58-68.
[19] L. Batista, U. Rabe, I. Altpeter, S. Hirsekorn, G. Dobmann, On the mechanism of nondestructive evaluation of cementite content in steels using a combination of magnetic Barkhausen noise and magnetic force microscopy techniques, Journal of Magnetism and Magnetic Materials, 354 (2014) 248-256.
[20] R. Hiramatsu, K.-J. Kim, T. Taniguchi, T. Tono, T. Moriyama, S. Fukami, M. Yamanouchi, H. Ohno, Y. Nakatani, T. Ono, Localized precessional mode of domain wall controlled by magnetic field and dc current, Applied Physics Express, 8 (2015) 023003.
[21] D. Ravelosona, D. Lacour, J. Katine, B. Terris, C. Chappert, Nanometer scale observation of high efficiency thermally assisted current-driven domain wall depinning, Physical review letters, 95 (2005) 117203.
[22] E. Beyer, L. Lahn, C. Schepers, T. Stucky, The influence of compressive stress applied by hard coatings on the power loss of grain oriented electrical steel sheet, Journal of Magnetism and Magnetic Materials, 323 (2011) 1985-1991.

[23] N. Chukwuchekwa, A.J. Moses, P. Anderson, Study of the effects of surface coating on magnetic Barkhausen noise in grain-oriented electrical steel, Magnetics, IEEE Transactions on, 48 (2012) 1393-1396.
[24] B. Betz, P. Rauscher, R. Harti, R. Schäfer, A. Irastorza-Landa, H. Van Swygenhoven, A. Kaestner, J. Hovind, E. Pomjakushina, E. Lehmann, Magnetization Response of the Bulk and Supplementary Magnetic Domain Structure in High-Permeability Steel Laminations Visualized In Situ by Neutron Dark-Field Imaging, Physical Review Applied, 6 (2016) 024023.
[25] H. Richert, H. Schmidt, S. Lindner, M. Lindner, B. Wenzel, R. Holzhey, R. Schäfer, Dynamic Magneto‐Optical Imaging of Domains in Grain‐Oriented Electrical Steel, steel research international, 87 (2016) 232-240.
[26] J. McCord, Progress in magnetic domain observation by advanced magneto-optical microscopy, Journal of Physics D: Applied Physics, 48 (2015) 333001.
[27] A. Hubert, R. Schäfer, Magnetic domains: the analysis of magnetic microstructures, Springer Science & Business Media, 2008.
[28] R. Grechishkin, S. Chigirinsky, M. Gusev, O. Cugat, N. Dempsey, G. Asti, L. Pareti, M. Ghidini, Magnetic Nanostructures in Modern Technology, in, Springer, 2008.
[29] D. Markó, I. Soldatov, M. Tekielak, R. Schäfer, Stray-field-induced Faraday contributions in wide-field Kerr microscopy and-magnetometry, Journal of Magnetism and Magnetic Materials, 396 (2015) 9-15.
[30] M. Frommert, C. Zobrist, L. Lahn, A. Böttcher, D. Raabe, S. Zaefferer, Texture measurement of grain-oriented electrical steels after secondary recrystallization, Journal of Magnetism and Magnetic Materials, 320 (2008) e657-e660.
[31] D. Dye, H. Stone, R. Reed, Intergranular and interphase microstresses, Current opinion in solid state and materials Science, 5 (2001) 31-37.
[32] L. Delannay, R.E. Logé, Y. Chastel, P. Van Houtte, Prediction of intergranular strains in cubic metals using a multisite elastic-plastic model, Acta materialia, 50 (2002) 5127-5138.
[33] S. Ding, G. Tian, G. Dobmann, P. Wang, Analysis of domain wall dynamics based on skewness of magnetic Barkhausen noise for applied stress determination, Journal of Magnetism and Magnetic Materials, 421 (2017) 225-229.